applied sciences

MDPI

Article

Impact of Wind Veer and the Coriolis Force for an Idealized Farm to Farm Interaction Case

Ola Eriksson [1,*], Simon-Philippe Breton [1,2], Karl Nilsson [1] and Stefan Ivanell [1]

[1] Department of Earth Sciences, Uppsala University, Wind Energy Campus Gotland, 621 67 Visby, Sweden; Simon-Philippe.Breton@geo.uu.se (S.-P.B.); Karl.Nilsson@geo.uu.se (K.N.); Stefan.Ivanell@geo.uu.se (S.I.)

[2] Environment and Climate Change Canada, 2121 Route Transcanadienne, Dorval, QC H9P 1J3, Canada

* Correspondence: Ola.Eriksson@geo.uu.se

Received: 25 January 2019; Accepted: 27 February 2019; Published: 5 March 2019

Abstract: The impact of the Coriolis force on the long distance wake behind wind farms is investigated using Large Eddy Simulations (LES) combined with a Forced Boundary Layer (FBL) technique. When using the FBL technique any mean wind shear and turbulent fluctuations can be added with body forces. The wind shear can also include the mean wind veer due to the Coriolis force. The variation of the Coriolis force due to local deviations from the mean profile, e.g., from wakes, is not taken into account in the FBL. This can be corrected for with an extra source term in the equations, hereon defined as the Coriolis correction. For a row of 4 turbines it is shown that the inclusion of the wind veer turns the wake to the right, while including the Coriolis correction turns it to the left. When including both wind veer and Coriolis correction the impact of wind veer dominates. For an idealized farm to farm interaction case, two farms of $4 * 4$ turbines with 6 km in between, it can be seen that when including wind veer and the Coriolis correction a approximately 3% increase in the relative production for a full wake direction can be seen and only a slightly smaller increase can be seen when including only wind veer. The results indicate that FBL can be used for studies of long distance wakes without including a Coriolis correction but efforts need to be taken to use a wind shear with a correct mean wind veer.

Keywords: long distance wake; farm to farm interaction; wind farm cluster; large Eddy simulations; LES; actuator disc; ACD; forced boundary layer; FBL; coriolis; wind veer

1. Introduction

The general trend for wind power shows an increase in installed capacity and a larger share offshore [1]. More and larger wind farms are planned offshore in Europe [2] and an increase in the number of wind farms that are built in close proximity in wind farm clusters can be seen [3].

This makes it interesting to study not only the wake interaction inside wind farms but also the long distance wakes behind wind farms and how the wake from one wind farm interacts with other wind farms, in a so-called farm farm interaction.

Studies of long distance wakes can be performed with different simulation methods ranging from self similar models, linearized models, Reynolds average Navier Stokes (RANS), Meso scale models (for example using the Weather Research and Forecasting model (WRF)) to Large Eddy Simulations (LES) [4–7]. WRF normally uses a lower grid resolution than LES, which makes it less computationally demanding but has therefore also the disadvantage that the wind farm needs to be more coarsely parameterized. WRF includes on the other hand more physics about the atmosphere. LES have the advantage that the higher resolution can resolve more scales in the flow and can more accurately model wake interaction especially inside the wind farms [8]. LES have led to good results for studying wakes inside wind farms, see, among others, [9–12]. LES have been used in fewer studies when it comes to long distance wakes and farm to farm interaction and are still challenging regarding the

needed computational resources. Earlier studies of long distance wakes have been performed for Horns Rev I [13] and Lillgrund [14]. In these studies the impact of the Coriolis force was not included and a wind shear with only a velocity in the streamwise direction was used. In a later study of the long distance wake behind Horns Rev I, the wind veer was included [8]. The wind veer was included as a mean value taken from a WRF simulation. When compared with the earlier study the results were closer to site data for the wake behind Horns Rev I.

The Coriolis force is in several LES studies using a forced boundary layer (FBL) technique not included in simulations [9,10]. With the larger distances involved in the study of long distance wakes the turn of the wind due to the Coriolis force becomes of higher importance. As the Coriolis force is proportional to the wind speed, it creates a directional change of the mean wind shear with height. Variations of this force in time and space also occur due to changes in wind speed associated to wind turbine's wakes and atmospheric turbulence. It is natural to question whether the turn of the wake is more greatly impacted by the mean wind veer or change in Coriolis force due to variations in velocity. This question was studied by Van der Laan [15] using RANS with the conclusion that the main impact was from the wind veer due to the downward momentum transport in the wake. For the studied latitude (43.3 deg) in the northern hemisphere it led to a turn to the right of the wake region. Van der Laan also looked at earlier studies of the Coriolis force in the northern hemisphere. The studies had different conclusions as to if the major impact is due to the reduction of the wind speed in the wake that turns the wake to the left or from the increased downward momentum transport due to the wind farm turning the wake to the right due to the wind veer. Some studies focused on the impact of wind veer and concluded that the farm wake turns to the right due to the wind veer. Other studies focused on the impact of the Coriolis force in the wake due to the reduced wind speed. One of the studies was performed with LES using a precursor simulation [16], this study indicated that a turn to the left dominated. These results gave a different conclusion than was found by Van der Laan [15]. Other studies found that the inclusion of the Coriolis force had some impact on the production for a full wake direction due to the turn of the wake [17].

The aim of the current study is to include the Coriolis force in simulations using a FBL technique. This is performed by including the mean wind veer in the FBL and combining it with a Coriolis correction for the deviations from the mean flow. The FBL technique used in this article gives you more control over the setup of the boundary layer, compared to a precursor simulation, since any mean wind profile can be added in the domain using body forces. This makes it possible to mimic for exempel a measured wind shear or a wind shear obtained from simulations using a Meso scale model. The wind shear can also include the mean wind veer due to the Coriolis force. A mean wind profile will however not take local deviations, e.g. from wakes and atmospheric turbulence, from the mean profile into account and therefore neglects a part of the Coriolis force. A correction for this neglection is proposed in this article which is also added as a source term, defined as the Coriolis correction.

The study will also examine the impact of the wind veer and the change in Coriolis force in the wake region on the development of the wake. The setup regarding wind veer and latitude is similar to Van der Laan [15] to be able to compare his results using RANS by these using LES. Using the FBL technique and the Coriolis correction also allows for the study of the impact of wind veer and local impact of the Coriolis force in the wake region independently. The results can be used to conclude if the Coriolis force needs to be considered for studies of long distance wakes and what needs to be included, i.e., the mean wind veer, the Coriolis correction or both. This is of importance to asses the results from studies using the FBL-technique without including the effects of the Coriolis force (for example [13,14]) or only including the wind veer (for example [8]). Further this study will investigate how the Coriolis force could impact the power output in a wind farm cluster.

2. Numerical Model

LES in the EllipSys3D code are used. LES resolve the largest and most energetic eddies and only the smallest eddies are modelled, here using the subgrid-scale model from Ta-Phouc [18].

The turbines are introduced into the simulations using an actuator disc method (ACD) based on airfoil data [19]. A generator-torque controller is used to adjust each turbine's rotational speed in the variable flow in a realistic way [20]. Both the ACD and the atmosphere i.e., turbulence and wind shear are introduced using body forces in the incompressible Navier Stokes (NS) equations formulated in vector notation, see Equation (1). In this equation $\mathbf{U}$ is the velocity, $\mathbf{P}$ the pressure, t the time, ρ the density of air and ν is the kinematic viscosity, and ν_{SGS} is the subgrid scale viscosity. The bar represent the filtered parameters. The coordinate system used in the article is $\mathbf{x} = (z, x, y)$ with the velocities $\mathbf{U} = (w, u, v)$ for the streamwise, spanwise and vertical directions. The body forces $\mathbf{f}$ that are added in the domain comes from the ACD ($\mathbf{f}_{ACD}$), from the FBL ($\mathbf{f}_{FBL}$) and from the turbulence ($\mathbf{f}_{turb}$) as described in [10]. The Coriolis correction defined in Equations (3) and (4) can be added as $\mathbf{f}_{Corr_{non}}$. The code is non-dimensional (normalized with respect to the rotor radius (R) and the undisturbed velocity at hub height (U_0)).

$$\frac{\partial \overline{\mathbf{U}}}{\partial t} + \overline{\mathbf{U}} \cdot \nabla \overline{\mathbf{U}} = -\frac{1}{\rho}\nabla \overline{\mathbf{P}} + \frac{1}{\rho}\mathbf{f}_{ACD} + \frac{1}{\rho}\mathbf{f}_{FBL} + \frac{1}{\rho}\mathbf{f}_{turb} + \mathbf{f}_{Corr_{non}} + \nabla\left[(\nu + \nu_{SGS}) * \nabla \overline{\mathbf{U}}\right], \quad \nabla \cdot \overline{\mathbf{U}} = 0 \quad (1)$$

The production (P) is calculated, according to Equation (2), as the angular velocity of the rotor (Ω_{rotor}), which adjust to the flow using the generator-torque controller, times the rotor torque. The rotor torque is calculated as the area integral over the rotor area (A) of the local forces in the tangential direction per unit area calculated in the ACD model ($f_{ACD_{\theta area}}$) times the local radius (r). In the results the relative production (P_{rel}) is presented which is P normalized with the production for the first turbine in the row of turbines (P_1).

$$P = \Omega_{rotor} \cdot \int \int_A f_{ACD_{\theta area}} r dA \quad (2)$$

2.1. The FBL Technique

The incoming neutral atmospheric boundary layer, which can also include a wind veer, is mimicked by using a FBL technique that uses body forces [11] to introduce the wind shear in the NS-equations, Equation (1). The body forces are calculated iteratively inspired by the immersed boundary technique in a prestep to reach the desired wind profile in the domain. In the main simulations these forces are applied in the whole domain to maintain the incoming wind shear in the whole domain. Varying body forces are similarly used to add a realistic atmospheric turbulence from the Mann model [21,22] as planes inside the equidistant region. The used method to impose the wind shear and the turbulence inside the domain has a number of advantages compared to the use of an initial flow condition and variations at the inlet boundaries [11]. Among others the applied wind shear is a solution to the NS-equations and the turbulence plane allows for a stretched region in the inlet of the domain which saves grid points for the equidistant region of interest (where the analysis are performed).

2.2. The Coriolis Correction

The Coriolis force due to the rotation of the Earth is proportional to the velocity and since the velocity differs with height this leads to a turning of the wind with height, a so-called wind veer. In the FBL the mean profile of the wind shear including wind veer is added using body forces. Deviation from the mean due to wakes and turbulence is not handled by the FBL and an extra Coriolis correction body force $\mathbf{f}_{Corr_{non}}$ needs to be added in Equation (1) to include this. Equations (3) and (4) show the added forces (before non-dimensionalization) associated to the Coriolis correction in the x respectively z directions. Here Ω is the rotation of the Earth, ϕ is the latitude, u, w are the instantaneous local velocities and U, W are the mean values used in the FBL. The latitude 43.3 degrees is used in the studied case which corresponds to the Coriolis parameter $f = 10^{-4}\ \frac{1}{s}$, also used by Van der Laan [15]).

The non dimensionalized (with respect to R and U_0) form, $\mathbf{f}_{Corr_{non}}$, of Equations (3) and (4) are added in Equation (1).

$$\mathbf{f}_{x,Corr} = -2 * \Omega * sin(\phi)(w - W) = -f * (w - W) \tag{3}$$

$$\mathbf{f}_{z,Corr} = 2 * \Omega * sin(\phi)(u - U) = f * (u - U) \tag{4}$$

3. Simulations

Simulations are performed for a row of turbines as well as for two idealized wind farms. The overall setup is similar to a study performed previously on the wake behind the Horns Rev wind farm [8], where U_0 = 8 m/s, with the same wind turbines (a downscaled version of the NREL 5 MW turbine corresponding to a Vestas V80 with rated power of 2 MW), with a hub height of 70 m and a R of 40 m. The simulations have a resolution (Δx) of 0.1 R (4 m) which has shown to be sufficient in earlier studies [10,23]. A non dimensionalized (with U_0 and R) time step (Δt) of 0.05 is used. In earlier studies using the FBL technique [8,10,11,23] a time step ranging between 0.025 and 0.05 have been used with stable results. All these time steps fulfil the CFL condition (which for Δx = 0.1 and u = 1 is fulfilled for Δt < 0.1). The turbulence box has a lower resolution 1.67 Δx and a larger time step of 0.12, therefore a spatial and temporal interpolation is employed. The total boundary layer height is 25 R (1000 m) and the grid has an equidistant area of 8 R in the vertical direction. The simulations ran first for 12,000 Δt to allow for the turbulence to advect through and fill the domain. All the turbines also need to adjust to the flow. The simulations thereafter continued to ran and the studied parameters are averaged for 12,000 Δt corresponding to 50 min in physical time. The boundary layers used are described below, followed by a further description of the used wind farm configurations and cases.

3.1. Boundary Layer

When using the FBL technique a mean wind shear and synthetic turbulence are added using body forces. Those are described below. Please recall that in the simulations neutral atmospheric conditions are assumed.

3.1.1. Wind Shear

The wind shear used in the simulations is a logarithmic profile for the horizontal velocity (U_{hor}) vs the height (y), see Equation (5). There (κ) is the von Karman constant and the roughness length is $z_0 = 10^{-4}$. The friction velocity u_* is calculated to provide a wind velocity of 8 m/s at hub height.

$$U_{hor}(y) = \frac{u_*}{\kappa} ln\left(\frac{y}{z_0}\right) \tag{5}$$

In the simulations two wind shear profiles are used, one with all flow in the streamwise direction and one with a turning of the wind with height.

Figures 1a–c provide information for the cases. Figure 1a shows the total horizontal velocity together with the corresponding streamwise component W when a linear wind veer of 2 degrees over the rotor is considered, as shown in Figure 1b. Figure 1c shows the spanwise velocity U corresponding to this case. For the former case where no wind veer is considered, U is the same as U_{hor} in Figure 1.

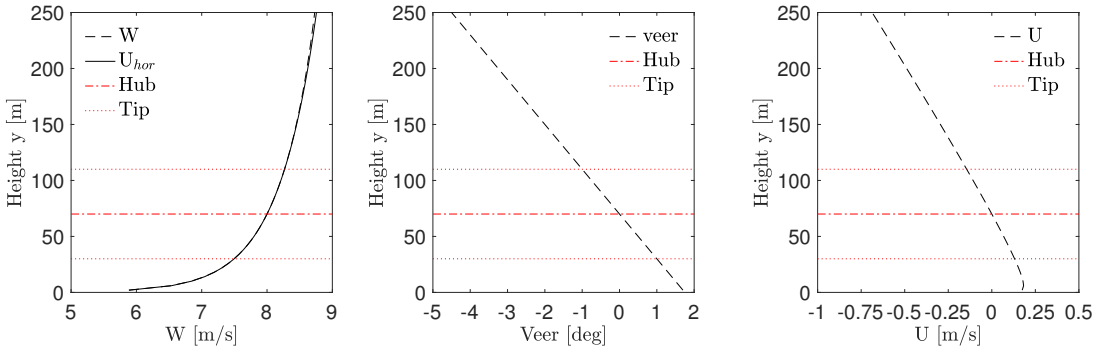

(**a**) (**b**) (**c**)

Figure 1. Used wind shears: (**a**) Streamwise velocity (W) for the case with wind veer and Horizontal velocity (U_{hor}) corresponding to the streamwise velocity when no veer is used. (**b**) Wind veer of 2 degrees over the rotor. (**c**) Spanwise velocity (U) for the case with wind veer. The horizontal red lines (Hub and Tip) show the heights covered by the rotor area.

3.1.2. Turbulence

The turbulence box has a length corresponding to 10 min in physical time used repeatedly. The side and vertical extensions are described below for each of the studied wind farm configurations.

The level of turbulence is based on the used $z_0 = 10^{-4}$, the same value used for the shear. This results, when adding the turbulence at 13 R, in a downstream development of the turbulence level (TI) (here defined as the standard deviation of the horizontal velocity divided by U_0) at hub height according to Figure 2. This simulation is performed in the grid for the row without any turbines. To avoid positioning the turbines in the first region where the turbulence level develops the most, as also seen in other studies [24], the first turbine is added at z = 100 R where the turbulence level is around 6 % according to Figure 2.

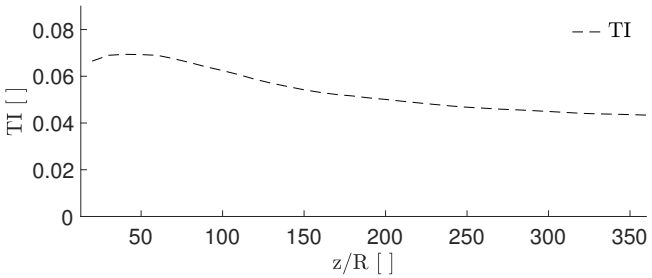

Figure 2. The development of the level of turbulence at hub height.

3.2. Wind Farm Configurations and Cases

Simulations are performed to study the flow behind a wind farm for a number of cases. This is to study how the wind farm wakes interact with other wind farms as well as how sensitive the simulations are to different wind shears and the turning of the wake due to the Coriolis force. Table 1 shows how the mean wind veer and the Coriolis correction are included in the studied cases. Simulations are performed in a first step for the flow behind a row of turbines and then for an idealized farm to farm interaction situation.

Table 1. Four cases are performed with different combinations of setup regarding mean wind shear and if a Coriolis correction is included.

Case:	ws	veer	ws cor	veer cor
Mean wind shear only in streamwise direction	X		X	
Mean wind shear including a wind veer		X		X
Coriolis correction is used			X	X

3.2.1. Row of Turbines

The row of turbines consists of four turbines with an internal spacing of 14 R, see Figure 3. The first turbine is at z = 100 R in the streamwise direction and at x = 50 R in the spanwise direction. The total domain has the extensions 100 R × 392 R × 25 R in the x , z respectively y directions. The inner equidistant region covers the x-coordinates 50 ± 17 R, the z-coordinates 10–392 R and has a height of 8 R. The extension of the equidistant region covers in the z-direction a distance up to 250 R (8 km) behind the last turbine of the row.

The turbulence is added at z = 13 R and has side extensions which cover with some margin the equidistant region, i.e., 38.4 R (covering 33–67 R in Figure 3). Vertically between 0.4 R and 10 R in height is added.

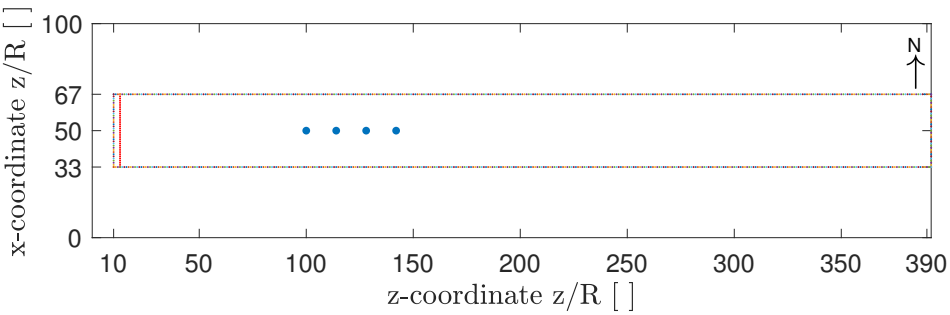

Figure 3. The placement of the turbines (•) in the the row in the LES domain covering 100 R × 392 R with an equidistant region (marked with the rectangle) of 34 R × 382 R. The turbulence is added at z = 13 R, at the red line.

3.2.2. Idealized Farm to Farm Interaction Case

Two idealized wind farms of 4 × 4 wind turbines with an internal spacing of 14 R are considered, see Figure 4. The first wind farm's front row turbines are placed at z = 100 R in the streamwise direction and are centered around x = 150 R in the spanwise direction. The total domain has the extensions 300 R × 392 R × 25 R in the x , z respectively y directions. The inner equidistant region covers the x-coordinates 150 ± 72.5 R, the z-coordinates 10–392 R and has a height of 8 R. The extension of the equidistant region covers in the z-direction the second wind farm that starts at 292 R, which corresponds to 150 R (6 km) behind the first wind farm.

The turbulence is added at z = 13 R and has side extensions which cover with some margin the equidistant region, i.e., 153.6 R (covering 77.5–222.5 R in Figure 4). Vertically between 0.4 R and 10 R in height is added.

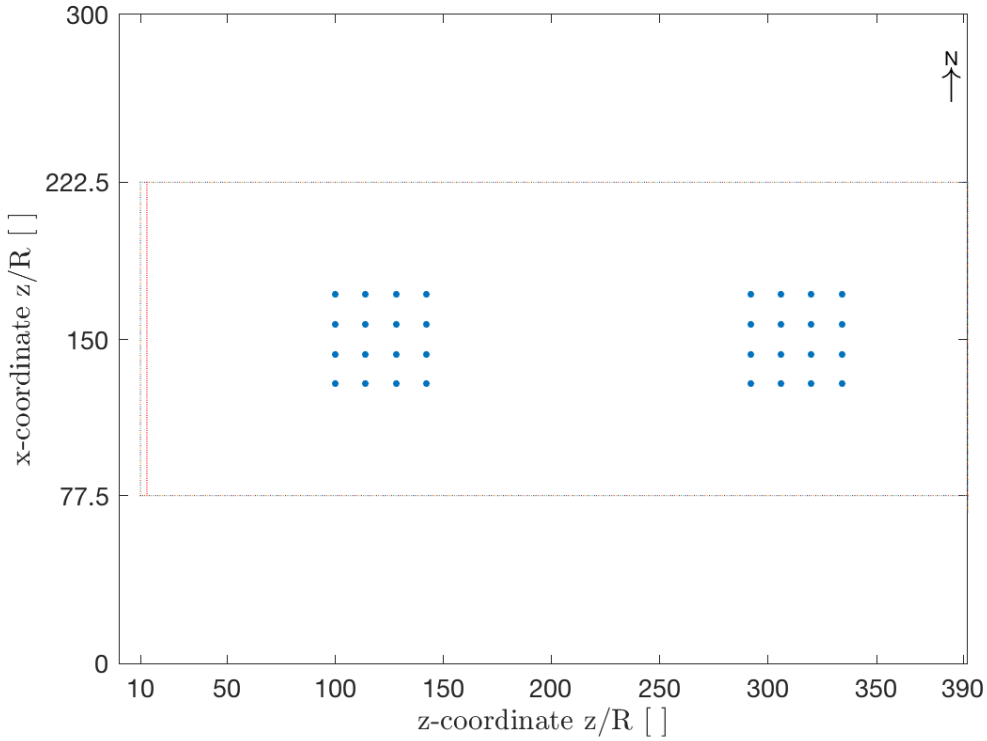

Figure 4. The placement of the turbines (•) in the two idealized wind farms in the LES domain covering 300 $R \times 392$ R with an equidistant region (marked with the rectangle) of 145 $R \times 382$ R. The turbulence is added at z = 13 R, at the red line.

4. Results and Discussion

First the flow behind the row of turbines is studied with the main focus being on the impact of the different cases in Table 1 on the streamwise and spanwise velocities in the long distance wake. Second an idealized farm to farm interaction case is studied with focus on how this could impact the overall energy production.

4.1. Impact of Wind Veer and Coriolis Correction on Long Distance Wakes

Studying the streamwise velocity, Figure 5, we can see the impact of the different configurations considered. The base case with no veer and no Coriolis correction can be seen in Figure 5a. Introducing the wind veer in Figure 5b a right turn of the wake can be seen while only including the Coriolis correction in Figure 5c shows a turn to the left. These results are those expected considering the used wind veer and the equations for the Coriolis correction. When including both the veer and Coriolis correction the resulting turn is to the right, indicating the dominating impact of the wind veer for the studied conditions. This result is further highlighted in Figure 6 that shows the contour lines of the streamwise velocity in the wake for the level 0.95. These results using LES are in line with the earlier findings from the study of Van der Laan [15] using RANS.

The spanwise component behind the row in Figure 7 is to the right if the wind profile includes a wind veer and otherwise it is around zero. This indicates that the major impact on the spanwise velocity is from a downward momentum transport from higher height. Inside the row, and at some distance behind, the spanwise components from the rotation of the wake behind each turbine can also be seen.

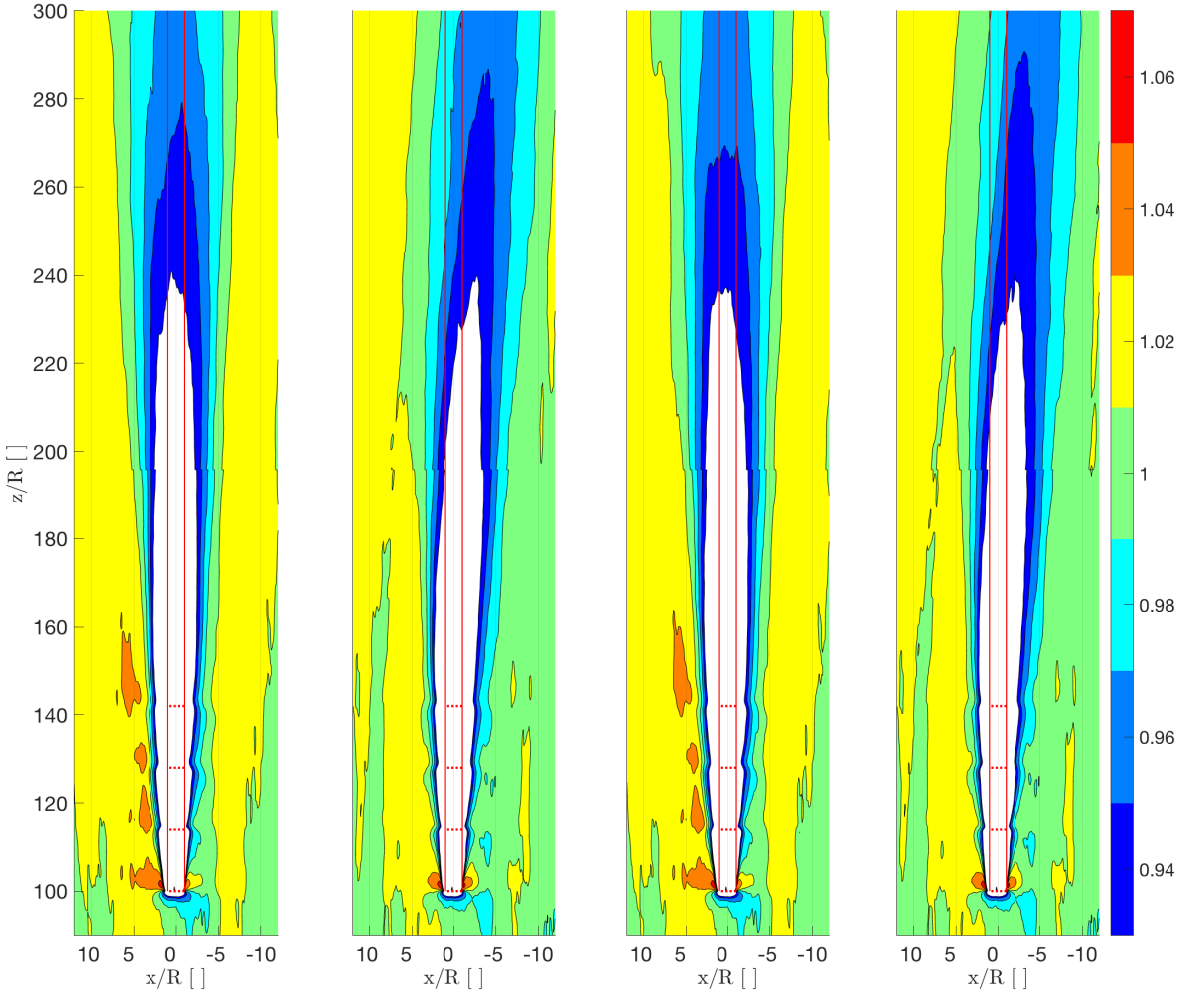

(**a**) (**b**) (**c**) (**d**)

Figure 5. Streamwise velocity (W) (see colorbar) at hub height for a row of turbines for cases: (**a**) ws (**b**) veer (**c**) ws cor (**d**) veer cor.

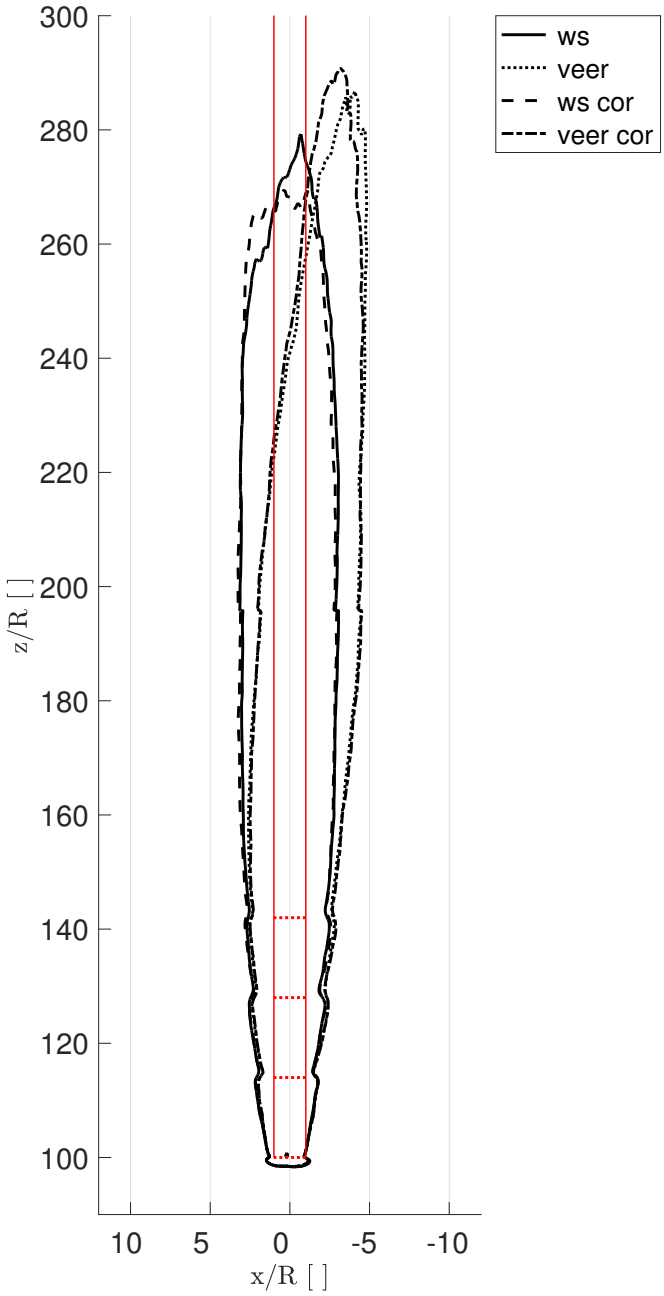

Figure 6. Contour lines of streamwise velocity (W) at hub height for a row of four turbines for the cases ws, veer, ws cor and veer cor shown for the level 0.95.

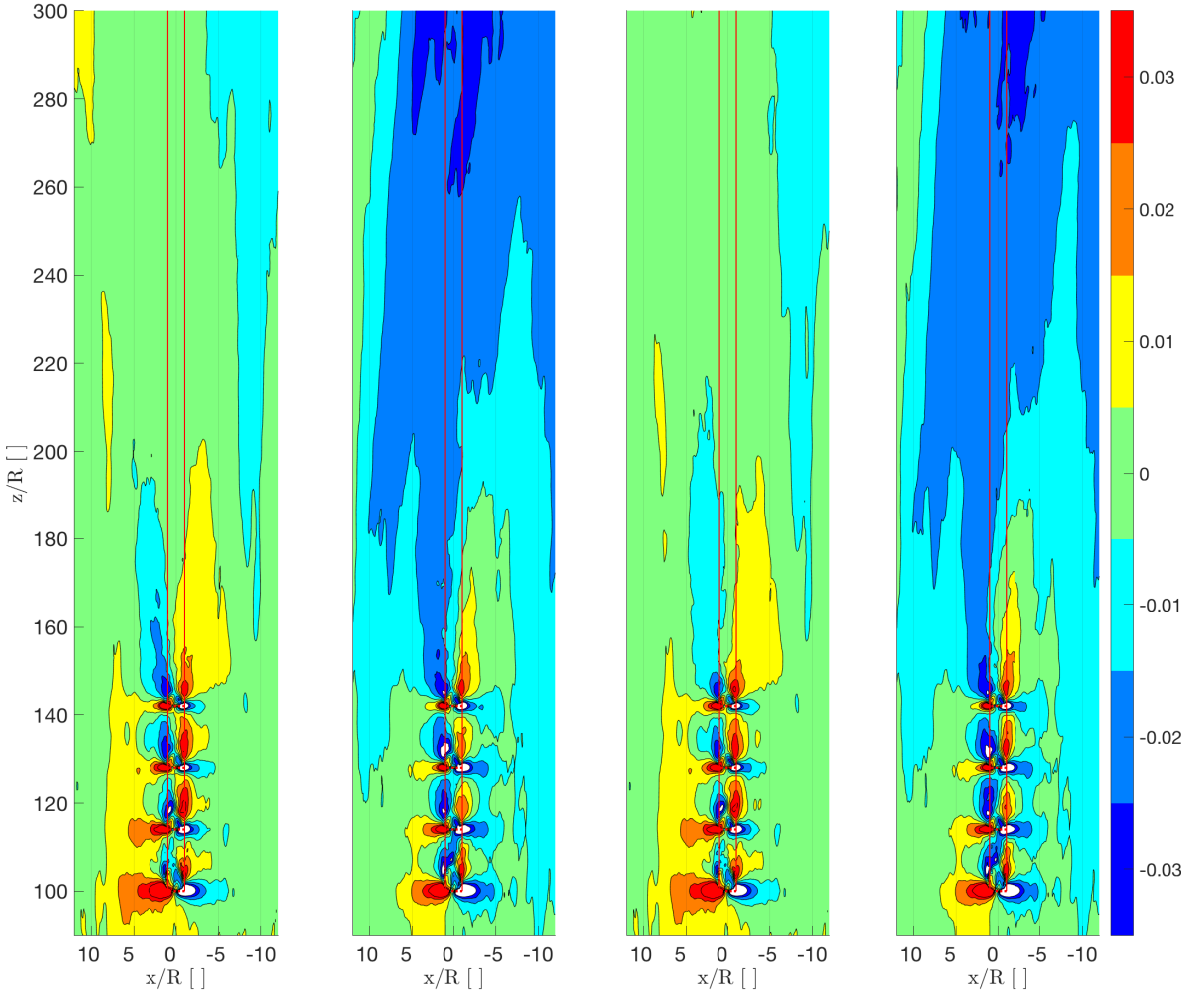

(**a**) (**b**) (**c**) (**d**)

Figure 7. Spanwise velocity (U) (see colorbar) at hub height for a row of turbines for cases: (**a**) ws (**b**) veer (**c**) ws cor (**d**) veer cor.

A simulation is also performed in the grid used to study a row of turbines but without turbines present for the case ws to study the development of the background flow. Part of the increased streamwise velocity outside the wake downstream in Figure 5 can be seen in the development of the background flow in Figure 8a. The background impact on the spanwise velocity is seen to be less important from a z position of about 100 R according to Figure 8b. In Figure 9 the difference with the background flow removed can be seen. The impact of the wind veer and Coriolis correction described above in Figure 5 is more clearly visible.

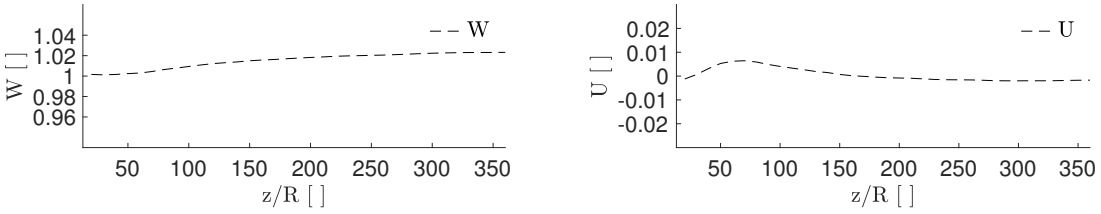

(**a**) (**b**)

Figure 8. The development of (**a**) streamwise velocity (W) (**b**) spanwise velocity (U) (mean over the equidistant region in x direction) at hub height, for case ws and no wind turbines.

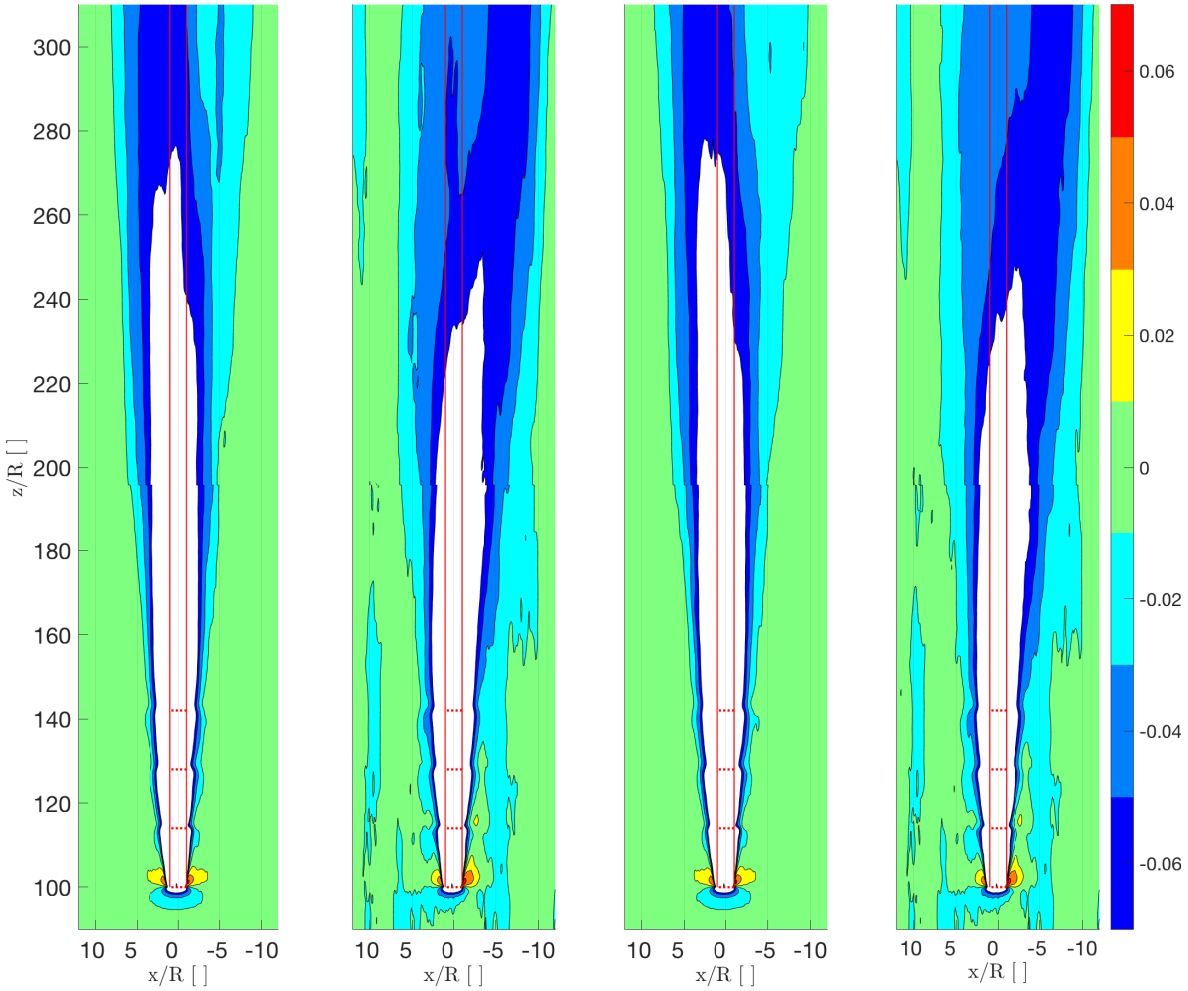

(**a**) (**b**) (**c**) (**d**)

Figure 9. Streamwise velocity (W) at hub height (see colorbar) with the background flow removed, for a row of turbines for cases: (**a**) ws (**b**) veer (**c**) ws cor (**d**) veer cor.

The relative production in Figure 10 shows a slightly faster recovery for turbine number two when including the wind veer and for turbine number four a slightly higher production value when including the Coriolis correction. The overall percental change in production for the whole row can be seen in Figure 11. Including both the wind veer and Coriolis correction increases the production by 1% compared to case ws. Looking at the individual impact of including either the wind veer or the Coriolis correction, it can be seen that the largest impact on the total production comes from the former.

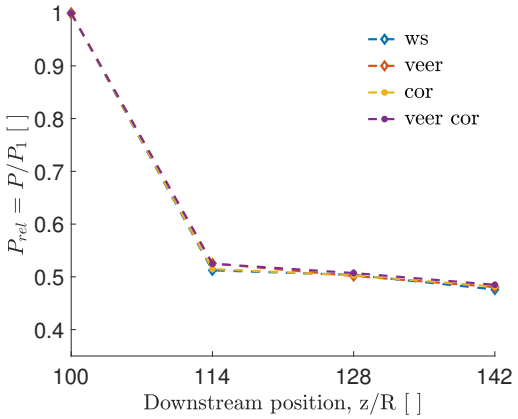

Figure 10. The relative production P_{rel} (Production (P) normalized with P for the first turbine in the row of turbines (P_1) for the different cases).

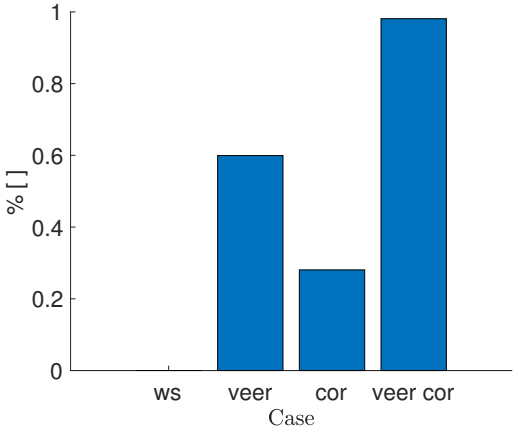

Figure 11. The percental change in production in comparison to case ws.

4.2. Impact on Energy Production for Farm to Farm Interaction Case

The velocity at hub height for case ws in the grid with two idealized wind farms can be seen in Figure 12a for the streamwise direction and in Figure 12b for the spanwise direction. The principle differences in a wake flow between the four different configurations (Table 1) are more easily seen behind the row of turbines, Figures 5 and 7, therefore only case ws is presented here.

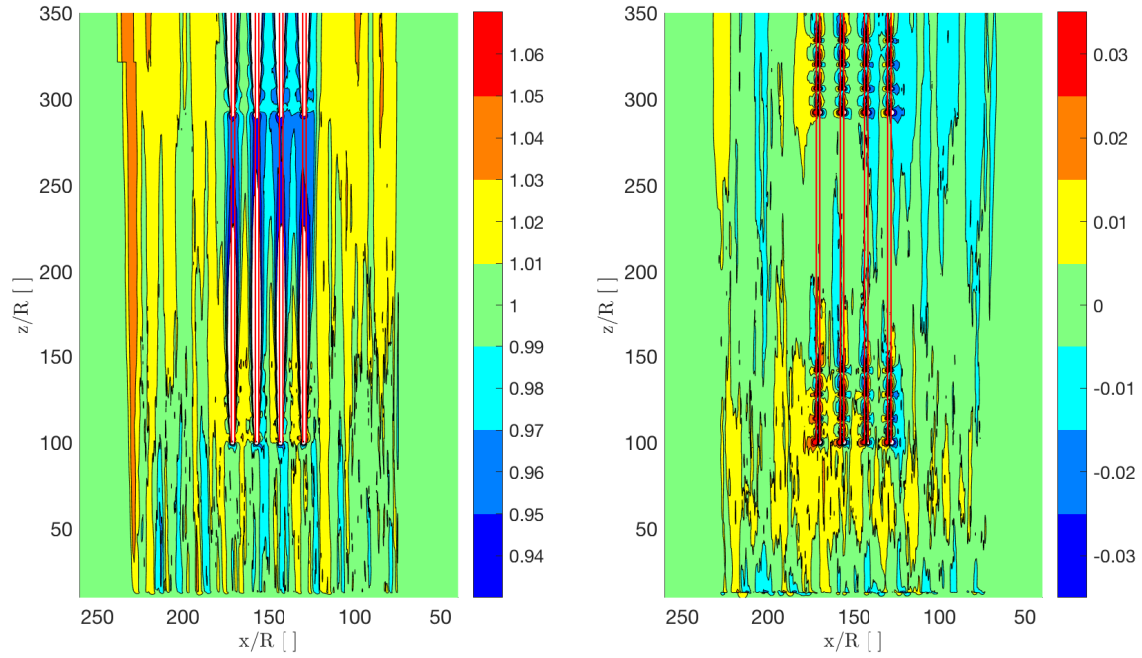

(**a**) (**b**)

Figure 12. Velocity (see colorbar) at hub height for two wind farms using case ws, for: (**a**) Streamwise direction (W) (**b**) Spanwise direction (U).

The relative production (mean for the four turbines for each line) for both the wind farms is shown in Figure 13. The impact of using the different configurations for the first wind farm is relatively small. For the second wind farm larger differences can be seen, the main impact coming from the inclusion of wind veer which leads to a higher production.

Looking at the relative production in more detail for the second wind farm compared to the first wind farm, see Figure 14a, it can be seen that with wind veer the relative loss in production for the second wind farm is less than 2% compared to around 7% for case ws. The impact from the considered Coriolis correction is smaller but in combination with wind veer it decreases the losses. The change in relative production for both wind farms compared to case ws can be seen in Figure 14b. When including the wind veer and Coriolis correction a total increase of around 3% can be seen compared to case ws for this full wake direction.

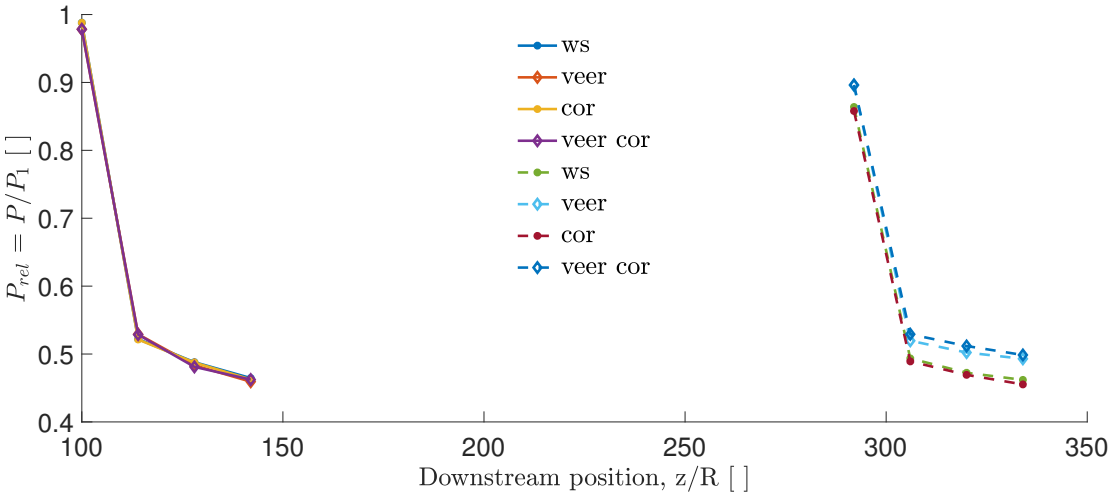

Figure 13. The relative production P_{rel} (Production (P) normalized with P for the first turbine in the row of turbines (P_1) per row for two wind farms for the different cases).

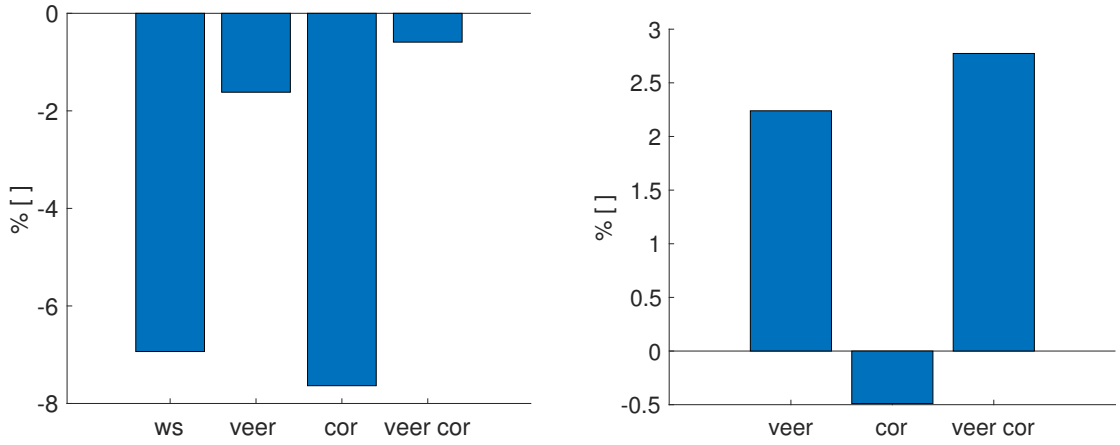

(**a**) (**b**)

Figure 14. Percental difference in production for the different configurations for (**a**) 2nd compared to 1st farm. (**b**) The total mean production compared to case ws.

5. Conclusions

LES using a FBL technique approach were performed for neutral atmospheric conditions with the Coriolis force included. The mean wind shear including the mean wind veer due to the Coriolis force can be included in the FBL. The variation of the Coriolis force due to the reduced velocity in the wake, the so-called Coriolis correction, was added with an extra force term. The study also examined the impact of the wind veer and the change in Coriolis force in the wake region on the development of the wake.

Including the wind veer in the simulation for a row of 4 turbines turns the wake behind it to the right and including the Coriolis correction turns it to the left. The implemented method shows the expected results considering the used wind veer and the equations for the Coriolis correction. When including both the veer and the Coriolis correction the resulting turn is to the right, indicating the dominant impact of the wind veer for the studied conditions. These results using LES are in line with the earlier findings from the study of Van der Laan [15] using RANS.

To study the impact of the Coriolis force on the total energy production in a wind farm cluster an idealized farm to farm interaction case was used. For a full wake direction in the idealized farm to farm interaction case it can be seen that when wind veer and the Coriolis correction are included relative production for a full wake direction increases by around 3%. This is only slightly less than when just wind veer is included. It can be noted that a lack of a yaw controller in the simulations could

suppress the increase of relative production. This is because the change of wind direction due to the Coriolis force could provide a smaller yaw misalignment than when no yaw controller is used.

To conclude, the FBL technique has been used including a wind veer and also a Coriolis correction. The results show that the Coriolis force impact on the mean wind shear (the wind veer) is greater when compared to its local impact due to the reduction of wind speed in the wake (here included as a so-called Coriolis correction). To include all aspects of the Coriolis force the implemented Coriolis correction can be used. The results indicate however that FBL technique can be used for studies of long distance wakes without including a Coriolis correction but efforts needs to be taken to use a wind shear with a correct mean wind veer. This is of importance to asses the results from earlier studies using the FBL-technique without including the effects of the Coriolis force or only including the wind veer.

In this study neutral atmospheric conditions were considered. The atmospheric conditions are expected to impact both the wind shear including the wind veer and the turbulence level which impact the recovery of the velocity in the wake. It could therefore be of interest for future work to investigate the relative impact of the different contributions of the Coriolis force in unstable and stable atmospheric conditions as well.

Author Contributions: Conceptualization, Methodology and Initial setup of simulations O.E. with contributions from K.N. and Supervision from S.-P.B. and S.I.; Simulations and Analysis O.E.; Writing Original Draft Preparation, O.E. with contributions of all authors to its review and editing; Supervision, S.-P.B. and S.I.; Project Administration and Funding Acquisition, S.I.

Funding: This research recieved no external funding.

Acknowledgments: The work was funded by the Vindforsk IV program. The computations were performed on resources provided by the Swedish National Infrastructure for Computing (SNIC) at the National Supercomputer Centre (NSC).

Conflicts of Interest: The authors declare no conflict of interest. The founding sponsors had no role in the design of the study; in the collection, analyses, or interpretation of data; in the writing of the manuscript, and in the decision to publish the results.

References

1. EWEA. *Wind in Power 2014 European Statistics*; EWEA: Brussels, Belgium, 2014.
2. EWEA. *European Wind Energy Association, Delivering Offshore Wind Power in Europe 2007*; EWEA: Brussels, Belgium, 2007.
3. Global Offshore Renewable Map-4c Offshore. Available online: https://www.4coffshore.com/offshorewind/ (accessed on 3 March 2019).
4. Brand, A. *Wind Power Plant North Sea–Wind Farm Interaction, The Effect of Wind Farming on Mesoscale Flow*; ECN: Petten, The Neatherlands, 2009.
5. Eriksson, O.; Ivanell, S. A survey of available data and studies of farm-farm interaction. In Proceedings of the EAWE PhD Seminar onWind Energy in Europe, Zurich, Switzerland, 12–13 September 2012.
6. Frandsen, S.; Barthelmie, R.; Rathmann, O.; Jørgensen, H.; Badger, J.; Hansen, K.; Ott, S.; Rethore, P.E.; Larsen, S.; Jensen, L. *Summary Report: The Shadow Effect of Large Wind Farms: Measurements, Data Analysis and Modelling*; Risø National Laborator: Roskilde, Denmark, 2007.
7. Hansen, K.S.; Réthoré, P.E.; Palma, J.; Hevia, B.G.; Prospathopoulos, J.; Peña, A.; Ott, S.; Schepers, G.; Palomares, A.; van der Laan, M.P.; et al. Simulation of wake effects between two wind farms. *J. Phys. Conf. Ser.* **2015**, *625*, 012008. [CrossRef]
8. Eriksson, O.; Baltscheffsky, M.; Breton, S.P.; Söderberg, S.; Ivanell, S. The Long distance wake behind Horns Rev I studied using large eddy simulations and a wind turbine parametrization in WRF. *J. Phys. Conf. Ser.* **2017**, *854*, 012012. [CrossRef]
9. Ivanell, S. Numerical Computations of Wind Turbine Wakes. Ph.D Thesis, KTH Engineering Sciences, Stockholm, Sweden, 2009.
10. Nilsson, K.; Ivanell, S.; Hansen, K.S.; Mikkelsen, R.; Breton, S.P.; Henningson, D. Large-eddy simulations of the Lillgrund wind farm. *Wind Energy* **2015**, *18*, 449–467. [CrossRef]

11. Troldborg, N.; Sørensen, J.N.; Mikkelsen, R.; Sørensen, N.N. A simple atmospheric boundary layer model applied to large eddy simulations of wind turbine wakes. *Wind Energy* **2014**, *17*, 657–669. [CrossRef]
12. Wu, Y.T.; Porté-Agel, F. Atmospheric turbulence effects on wind-turbine wakes: An LES study. *Energies* **2012**, *5*, 5340–5362. [CrossRef]
13. Eriksson, O.; Mikkelsen, R.; Nilsson, K.; Ivanell, S. Analysis of long distance wakes of Horns rev 1 using actuator disc approach. *J. Phys. Conf. Ser.* **2012**, *555*, 012032. [CrossRef]
14. Eriksson, O.; Lindvall, J.; Breton, S.P.; Ivanell, S. Wake downstream of the Lillgrund wind farm—A Comparison between LES using the actuator disc method and a Wind farm Parametrization in WRF. *J. Phys. Conf. Ser.* **2015**, *625*, 012028. [CrossRef]
15. Van der Laan, M.P.; Sørensen, N.N. Why the Coriolis force turns a wind farm wake clockwise in the Northern Hemisphere. *Wind Energy Sci.* **2017**, *2*, 285–294. [CrossRef]
16. Allaerts, D.; Meyers, J. Gravity Waves and Wind-Farm Efficiency in Neutral and Stable Conditions. *J. Bound.-Layer Meteorol.* **2018**, *166*, 269–299. [CrossRef]
17. Argyle, K. Computational Fluid Dynamics Modelling of Wind Turbine Wake Losses in Large Offshore Wind Farms, Incorporating Atmospheric Stability. Ph.D. Thesis, Loughborough University, Loughborough, UK, 2014.
18. Ta Phuoc, L. *Modéles de Sous Maille Appliqués Aux éCoulmements Instationnaires Décollés*; Tech. Rep. LIMSI 93074; LIMSI: Orsay, France, 1994.
19. Mikkelsen, R. *Actuator Disc Methods Applied to Wind Turbines*; DTU: Lyngby, Denmark, 2003.
20. Breton, S.P.; Nilsson, K.; Ivanell, S.; Olivares-Espinosa, H.; Masson, C.; Dufresne, L. Study of the effect of the presence of downstream turbines on upstream ones and use of a controller in CFD wind turbine simulation models. *J. Phys. Conf. Ser.* **2012**, *555*, 012014. [CrossRef]
21. Mann, J. *Wind Field Simulation*; Risø National Laborator: Roskilde, Denmark, 1998.
22. Mann, J.; Ott, S.; Jørgensen, B.H.; Frank, H.P. *WAsP Engineering 2000*; Risø National Laborator: Roskilde, Denmark, 2013.
23. Eriksson, O.; Nilsson, K.; Breton, S.P.; Ivanell, S. Analysis of long distance wakes behind a row of turbines–A parameter study. *J. Phys. Conf. Ser.* **2014**, *555*, 012032. [CrossRef]
24. Keck, R.-E.; Mikkelsen, R.; Troldborg, N.; de Maré, M.; Hansen, K.S. Synthetic atmospheric turbulence and wind shear in large eddy simulations of wind turbine wakes. *Wind Energy* **2014**, *17*, 1247–1267. [CrossRef]